J. Pharm. Pharmacol. 1981, 33: 129–135
Received September 1, 1980

0022–3573/81/030129–07 $02.50/0

The effect of compression on the capillary microstructure of tablets*

F. CARLI**, I. COLOMBO**, L. SIMIONI† AND R. BIANCHINI

Ricerca e Sviluppo Farmaceutico, Farmitalia Carlo Erba, Via Imbonati 24, Milano, Italy

The effect of compaction pressure on the capillary characteristics of compacts of a crystalline drug and of a pure polymer was studied by means of penetration and porosimetry measurements. Not only the constant but also the exponent m of the general penetration volume-time relationship $V = K^m t^m$ proved to be strongly dependent on the pressure: as the compaction pressure is increased, the value of m tends to decrease. The capillary penetration data also showed the development of a marked heterogeneity in the structure of the polymer compacts at the lower compaction pressures: at these pressures the surface layers showed a much lower penetrability than the inner core of the compacts, whereas at the higher pressures the structure of the compacts was homogeneous. Furthermore, on the basis of a generally used equation describing the powder consolidation process, it was possible to relate the most relevant variation of the kinetics of capillary penetration into the drug compacts to the deformation of the particles. It is concluded that the capillary penetration measurements can give useful information in the understanding of the behaviour of pharmaceutical powders under compression.

Since the work of Nogami et al (1963) and Ganderton (1969), much research has been carried out in the pharmaceutical field to study liquid penetration into compressed tablets or into powder beds (Samyn & Yung 1970; Sixsmith 1977; Ahmed & Enever 1978; Lerk et al 1979). All the researchers applied the classical Washburn (1921) equation:

$$L^{1/m} = R\gamma \cos\theta \, t/2\eta \quad .. \quad (1)$$

where: L = length of penetration, γ = surface tension of liquid, θ = solid/liquid contact angle, t = time, η = liquid viscosity, m = 0·5.

In many cases the length of penetration was replaced with the volume of penetration, but m was always considered equal to 0·5.

Equation (1) can be written in a simplified form as:

$$V = K^m t^m \quad .. \quad .. \quad (2)$$

which can also be written in a logarithmic form as

$$\log V = K' + m \log t \quad .. \quad (3)$$

where: V = volume of penetration, K and K′ = constant, t = time, m = numerical factor (0·5).

Only recently Carli & Simioni (1979) have drawn attention to the fact that m can assume values other than 0·5.

Furthermore, values of m other than 0·5 have also been reported by authors operating in many unrelated fields of research such as: (a) moisture flow through the soil (Rode 1969); (b) liquid penetration into paper (Hoyland & Field 1976); (c) liquid flow into beds of inorganic powders (Heertjes & Kossen 1967; Schicketanz 1974).

However, it has been argued that the value of m for the penetration into compressed tablets is effectively 0·5 (Groves & Alkan 1979).

It is our object to demonstrate the existence of m values other than 0·5 also for the penetration process into compressed tablets and to show that interesting information on the mechanism of powder compression can be obtained by capillary penetration measurements.

MATERIALS AND METHODS

Materials

The powders used were the 250–200 μm fraction of a crystalline drug (a weak organic acid with antilipolytic activity, Farmitalia Carlo Erba, Italy), melting point between 188 and 190 °C, and the copolymer of vinylchloride and vinylacetate (Sicron 822, Montedison, Italy), with a glass transition temperature of 75 °C (Mod. DSC 2, Perkin Elmer,

* Presented at the British Technology Conference, London, April, 1980.
** Correspondence.
† Present address: Ind. Pharm., Gruppo Lepetit, via Durando 38, Milano, Italy.

USA), 80% by weight between 125 and 40 μm (Alpine 200 Air Jet Sieve, Alpine, Germany).

The densities of the powders, measured with a helium pycnometer (Beckman, USA), were respectively 1·45 g ml^{-1} (drug) and 1·30 g ml^{-1} (polymer). The water contact angle (Wettability Tester, Lorentzen-Wettre, Sweden) was 50° for the drug and 78° for the polymer.

Methods

Tablets were prepared by compressing 0·5 g of the powders on a single flat punch press (Nassovia, Germany), instrumented with piezo-electric load washers (Kistler, Switzerland). The responses of the instrumentation were recorded on an ultraviolet oscillograph (Southern Instruments, Mitcham). Before each compression, the surfaces of the die were lightly brushed with a 2% w/w solution of stearic acid in 1:1 solution of carbon tetrachloride and acetone. The apparent densities of the finished tablets were determined on at least ten tablets from their measured weights and dimensions. The tablets were stored in controlled humidity conditions for 24 h before testing.

Capillary penetration measurements were made at 25 °C using a simple apparatus (Couvreur et al 1976). Distilled water for the polymer compacts and distilled water saturated with the drug for the drug compacts were used as penetration liquids. All the measurements were made in 3–4 replicates.

Total pore volume and pore size distributions were determined using a mercury porosimeter model 225 (Carlo Erba Strumentazione, Italy), with maximum penetration pressure of 196 MN m^{-2} and introducing three tablets into the sample compartment. All the measurements were carried out in duplicate.

RESULTS AND DISCUSSION

Drug compacts

Fig. 1 and Table 1 show the effect of compression on the penetration of water into the compacts of the crystalline drug. The penetration volume data are plotted on a double logarithmic scale according to equation (3).

After an initial re-equilibration period, all the curves show a linear region, which covers more than 70% of the overall volume of penetration. To prove that the initial non-linear penetration region was simply due to a re-equilibration process and not to the presence of surface layers with a capillary structure different from the core of the compacts, we carefully scraped about one-third w/w from the surface and measured the penetration: superimposable curves were obtained.

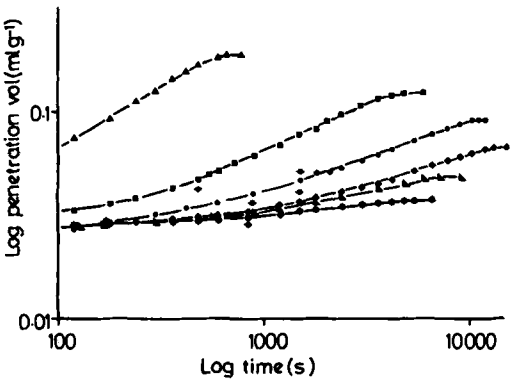

FIG. 1. Effect of compaction pressure on the water capillary penetration into the crystalline drug compacts: ▲, 32 MN m^{-2}; ■, 96·8 MN m^{-2}; ●, 142·0 MN m^{-2}; ◆, 214·3 MN m^{-2}; ◣, 366·6 MN m^{-2}; ✱, 508·3 MN m^{-2}. Each experimental point is the mean of 3–4 replicates (c.v. ≤ 10%). Arrows mark the onset of linear sections. When tablets are placed on the filter of the apparatus, an instantaneous apparent volume of 0·03 ml g^{-1} is registered, probably due to surface spreading; this is followed by a lag time, progressively prolonging as compaction is increased, before actual penetration takes place.

The linear region was identified by carrying out a least squares analysis of data (Snedecor 1964): the values of m of equation (3), derived from the slopes of these linear regions, are reported in Table 1, together with the correlation coefficients r, which were always significant at $P < 0{\cdot}001$.

As the compaction pressure is increased from 32·0 MN m^{-2} to 508·3 MN m^{-2} the value of m is lowered from 0·59 to 0·095. An analysis of variance (Winer 1962) of the mean m values showed that they differ with a high level of significance ($F = 43{\cdot}07$, at $P < 0{\cdot}001$, group d.f. = 5, error d.f. = 14).

Table 1. Effect of compaction pressure on water capillary penetration into the crystalline drug compacts. (m = exponent of equation (2); r = correlation coefficient of data in the linear region; K = constant of equation (2); r and m derived by least square analysis, K by inserting m values into equation (4).

Compaction pressure MN m^{-2}	m	r[b]	K $\frac{\text{ml}^{1/m}}{\text{g}^{1/m} \times \text{s}}$
32·0	0·590 ± 0·030[a]	0·9460 (30)[c]	1·0 × 10^{-3}
96·8	0·459 ± 0·007	0·9677 (22)	2·6 × 10^{-5}
142·0	0·364 ± 0·005	0·9738 (22)	1·0 × 10^{-7}
214·3	0·314 ± 0·002	0·9789 (22)	7·1 × 10^{-9}
366·6	0·292 ± 0·032	0·8751 (22)	2·0 × 10^{-9}
508·3	0·095 ± 0·011	0·7707 (26)	1·0 × 10^{-17}

a = Standard error.
b = at $P < 0{\cdot}001$.
c = d.f.

The constant K for each compaction pressure was calculated by inserting the found values of m in the following expression, derived from equation (3):

$$\log K = \frac{K^1}{m} \quad .. \quad .. \quad .. \quad (4)$$

where K^1 is simply the intercept value (at t = 1 s) of equation 3 derived by least squares analysis. As shown in Table 1, K progressively decreases, with the most relevant reduction occurring when the compaction pressure is raised from 366·6 MN m^{-2} to 508·3 MN m^{-2}.

The cumulative pore volume distribution and the pore size distribution function (Orr 1969/70) derived by mercury porosimetry measurements are shown in Fig. 2. The increase of compaction pressure from 32·0 up to 508·3 MN m^{-2} leads to about a ten-fold reduction in the total pore volume (from 0·167 ml g^{-1} to 0·015 ml g^{-1}) and a marked shifting of the pore size distribution towards the smaller pores.

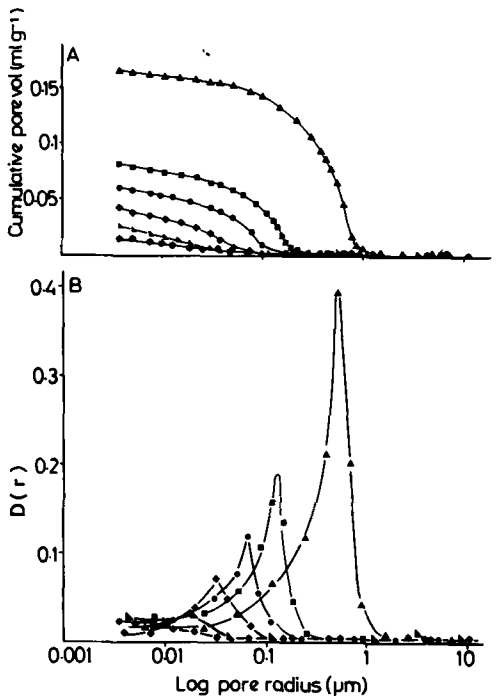

FIG. 2. The effect of compaction pressure on the cumulative pore size distribution (upper plot) and pore size distribution function (lower plot) of the drug compacts. ▲, 32 NM m^{-2}: ■, 98·8 MN m^{-2}; ●, 142·0 MN m^{-2}; ◆, 214·3 MN m^{-2}; ◣, 366·6 MN m^{-2}; ✳, 508·3 MN m^{-2}. Ordinates: cumulative pore volume, ml g^{-1} (A), D(r) = dV/d (log r), distribution function, ml g^{-1} (B).

Furthermore the increase of compaction pressure changes the shape of the pore size distribution, which changes from a well-defined, narrow unimodal character to a wide, poorly-defined character; in fact, at 32·0 MN m^{-2} compaction pressure a sharp peak is detectable at around 0·5 μm, whereas no peak can be identified at 508·3 MN m^{-2} compaction pressure.

If we compare these pore structure data with the penetration results, we observe that low m and K values seem to be related to a microstructure characterized by a very wide pore size distribution, shifted towards the smallest pores, whereas high m and K values seem to be related to well-defined and narrow pore size distribution, shifted towards the largest pores. Further information on the evolution of the microstructure of the drug powder under compression can be gained by comparing the values of the total pore volume measured by three different techniques (density measurements, mercury porosimetry, capillary penetration), as shown in Table 2.

Table 2. Effect of compaction pressure on crystalline drug compact void volumes determined by three different techniques: V_T, the theoretically available void volume, derived by the true (ρ_t) and apparent densities (ρ_a) of compacts: $V_T = 1 - (\rho_a/\rho_t)$; V_{Hg}, the pore volume measured by mercury porosimetry; V_{H_2O}, the final volume of water capillary saturation.

Compaction pressure MN m^{-2}	V_T ml g^{-1}	V_{Hg} ml g^{-1}	V_{H_2O} ml g^{-1}
32·0	0·172 ± 0·002[a]	0·167 ± 0·004[a]	0·160 ± 0·003[a]
96·8	0·076 ± 0·001	0·082 ± 0·002	0·096 ± 0·006
142·0	0·057 ± 0·001	0·061 ± 0·002	0·062 ± 0·004
214·3	0·045 ± 0·002	0·042 ± 0·001	0·033 ± 0·003
366·6	0·034 ± 0·001	0·026 ± 0·001	0·020 ± 0·003
508·3	0·028 ± 0·003	0·015 ± 0·002	0·007 ± 0·001

a = Standard error.

There is a general good agreement between the various techniques, the only exception being the values at the higher compaction pressures: at 508·3 MN m^{-2} the mercury porosimetry indicated a pore volume 50% lower than the one calculated by the true and apparent densities of the compacts, with the volume saturated by water being only 25% of the total theoretically available. These results indicate that at higher compaction pressures a high percentage of pores smaller than 0·037 μm, the lowest pore radius detectable by the porosimeter, are formed and that most of the pores are probably blind, so that water cannot fully penetrate them. The Heckel (1961) plot of the drug powder consolidation data is shown in Fig. 3: the initial curved section up to a compaction pressure of about

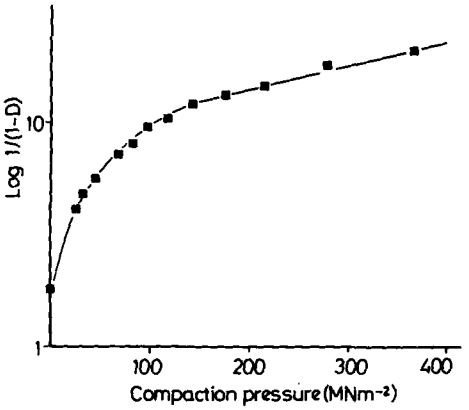

FIG. 3. Heckel plot of the crystalline drug powder consolidation data. Relative density, D, is calculated by dividing the density of the tablet by the true density of the drug powder. Each experimental point is the mean at least of 10 replicates (c.v. < 1%).

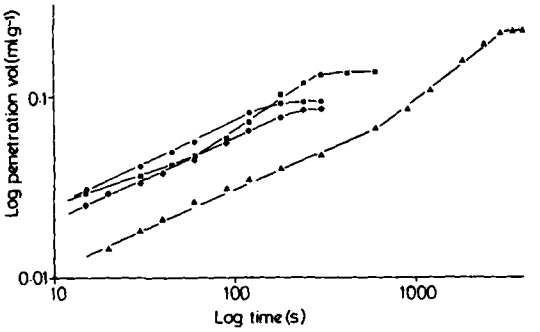

FIG. 4. Effect of compaction pressure on the water capillary penetration into the polymer compacts: ▲, 53·6 MN m^{-2}; ■, 87·9 MN m^{-2}; ●, 176·3 MN m^{-2}; ✱, 441·2 MN m^{-2}. Each experimental point is the mean of 3–4 replicates (c.v. ≤ 10%).

140 MN m^{-2} can be related to particle rearrangement, whereas the following linear region can be considered due to plastic deformation and/or fragmentation of particles.

The value of the mean yield pressure derived by the reciprocal of the slope of the linear region (Hersey & Rees 1970) was 402·7 MN m^{-2}. This result tends to suggest that when the compaction pressure is raised to values around or above 400 MN m^{-2} the drug particles undergo plastic flow and/or fracture, leading to a compact texture of small and blind pores, as indicated also by the dramatic reduction of the capillary penetration constant K and the changes of the pore size distribution.

Polymer compacts

Fig. 4 shows the effect of compression on the penetration of water into the polymer compacts. The most relevant observation to be made is that the compacts prepared at the lowest compaction pressure (53·6 MN m^{-2}) present two linear regions, with markedly different slopes, and that their final saturation requires much longer than the other compacts.

Also the compacts at 87·9 MN m^{-2} show a penetration curve with two definite linear sections, but the final saturation is fully achieved in a much shorter time, comparable to the saturation times of the compacts prepared at the higher pressures.

The initial linear region with lower slope is not present in the compacts prepared at the higher compaction pressures (176·3 and 441·2 MN m^{-2}), which exhibit a penetration curve with only one slope up to the final saturation of the compacts.

The parameters of the least square analysis of the penetration data are reported in Table 3.

As the compaction pressure is increased, the m value is progressively decreased; for the compacts exhibiting two linear sections both the m values are reduced.

An analysis of variance of the mean m values showed that they differ with a high level of significance ($F = 6·9$, at $P < 0·001$; group d.f. = 5; error d.f. = 16), confirming that compaction pressure exerts a strong influence on the slopes of the double logarithmic penetration curves.

In Table 3 are also reported the K values, derived by inserting the found values of m into equation 4: K for the two initial regions of the compacts prepared at 53·6 and 87·9 MN m^{-2} is smaller than all the other values of the penetration constant, but in all cases the effect of the compaction pressure on

Table 3. Effect of compaction pressure on water capillary penetration into the polymer compacts. (m = exponent of equation (2); r = correlation coefficient of data in the linear region; K = constant of equation (2); r and m derived by least square analysis, K by inserting m values into equation (4).

Compaction pressure MN m^{-2}	m	r^d	K ml^1/m g$^{1/2}$/m × s
53·6	0·452^a ± 0·040^c	0·9234 (25)^e	4·4 × 10^{-6}
	0·799^b ± 0·071	0·8677 (19)	5·0 × 10^{-5}
87·9	0·331^a ± 0·054	0·7560 (14)	2·2 × 10^{-6}
	0·701^b ± 0·116	0·8709 (18)	1·7 × 10^{-5}
176·3	0·472 ± 0·019	0·9301 (18)	3·8 × 10^{-5}
441·2	0·451 ± 0·038	0·8488 (26)	3·3 × 10^{-5}

c = Standard error.
a and b = derived by the slope of the first (a) and second (b) section of the double logarithmic plot of penetration data.
d = at $P < 0·001$.
e = d.f.

the K values for the polymers is very much less pronounced than that found for the drug compacts.

To investigate the cause of the two-slope penetration curves for the compacts prepared at the lower compaction pressures we carefully scraped about one third w/w from the surface of the compacts and measured the penetration rate: the resulting curves exhibited only one slope, not significantly different from the second one observed on the unscraped compacts. This result proved the existence of tablet surface layers having a penetrability effectively different from the core of the tablet.

The mercury porosimetry data, shown in Fig. 5, were corrected for the compressibility of the material (Palmer & Rowe 1974; Colombo & Carli, unpublished data 1980). As the compaction pressure is raised from 53·6 up to 441·2 MN m^{-2}, the total pore volume is decreased from 0·220 to 0·051 ml g^{-1} and the peak of the pore size distribution is shifted from 6 to 3 μm. All the pore size distributions show a well-defined unimodal character, even at the higher compaction pressure.

If we compare the total pore volumes measured with the three different techniques (see Table 4) as previously done for the crystalline drug compacts,

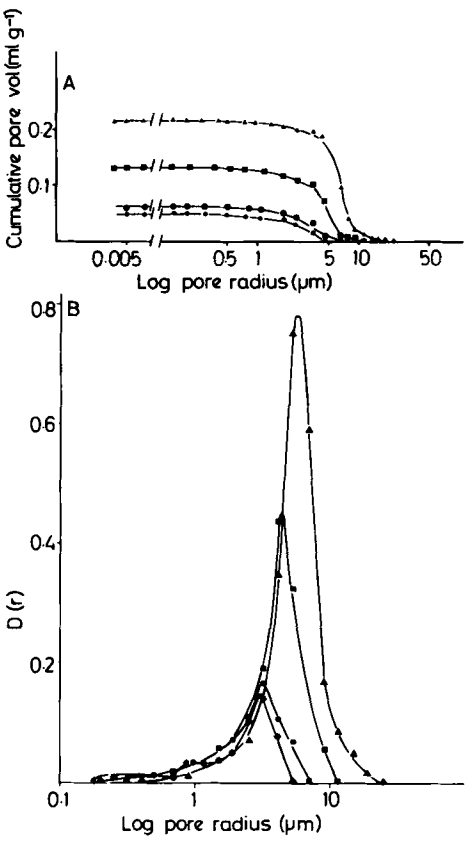

FIG. 5. The effect of compaction pressure on the cumulative pore size distribution (upper plot) and pore size distribution function (lower plot) of the polymer compacts: ▲, 53·6 MN m^{-2}; ■, 87·9 MN m^{-2}; ●, 176·3 MN m^{-2}; ✱, 441·2 MN m^{-2}. Ordinate: Cumulative pore volume, ml g^{-1} (A) D(r) = dV/d (log r), distribution function ml g^{-1} (B).

Table 4. Effect of compaction pressure on polymer compact void volume determined by three different techniques: V_T, the theoretically available void volume, derived by the true (ρ_t) and apparent densities (ρ_a) of compacts: $V_T = 1 - (\rho a/\rho t)$; V_{Hg}, the pore volume measured by mercury porosimetry; V_{H_2O}, the final volume of water capillary saturation.

Compaction pressure MN m^{-2}	V_T ml g^{-1}	V_{Hg} ml g^{-1}	V_{H_2O} ml g^{-1}
53·6	0·292 ± 0·003[a]	0·220 ± 0·008[a]	0·230 ± 0·020[a]
87·9	0·167 ± 0·001	0·136 ± 0·005	0·138 ± 0·007
176·3	0·102 ± 0·001	0·067 ± 0·002	0·096 ± 0·005
441·2	0·083 ± 0·001	0·051 ± 0·002	0·087 ± 0·005

a = Standard error.

we can observe that there is generally good agreement between the volumes of water saturation and the void volumes derived by the true and apparent densities of the compacts. Water seems to be able to saturate all the theoretically available pores (80% at the lower compaction pressures, 100% at the higher), differently from the drug compacts, which exhibited, at the highest compaction pressure, only a 25% water saturation level. This suggests that the compaction of the polymer does not lead to the massive formation of blind and/or closed pores. The mercury total pore volumes are always lower than those derived by the true and apparent densities of the compacts: this could be due to the presence of pores smaller than those detectable at the highest mercury intrusion pressure.

The Heckel plot of the polymer compression data is shown in Fig. 6: there is only one initial linear region from 0 to 87·9 MN m^{-2}, suggesting densification by plastic deformation, with no particle rearrangement (York & Pilpel 1973). Since the glass transition temperature of the polymer is low, 75 °C, densification of the polymer can take place also by viscous flow at the points of contact between the particles. This mechanism can be considered similar to the asperity melting found by York & Pilpel (1973) on low melting point fatty acids.

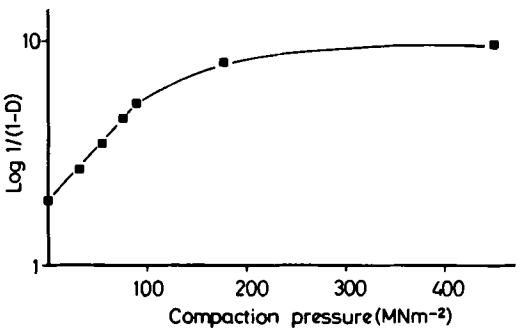

FIG. 6. Heckel plot of the polymer powder consolidation data. Relative density, D, is calculated by dividing the density of the tablet by the true density of the polymer powder. Each experimental point is the mean at least of 10 replicates (c.v. $\leqslant$ 2%).

The value of the mean yield pressure derived by the reciprocal of the slope of this linear section (Hersey & Rees 1970) was about 87·2 MN m^{-2}.

At compaction pressures above the mean yield pressure the polymer compacts exhibit a homogeneous capillary microstructure (water penetrates the whole compact at the same rate), whereas at pressures below this value the outer layers of the compacts offer a lower penetrability than the inner core. A tentative explanation may lie in considering that at these lower compaction pressures, stress is particularly concentrated on the surface layers, being only partially transmitted by the not-yet deforming particles to the inner core of the compact. This may bring about a temperature rise in the surface portion of the compact, with viscous flow of polymer at the interparticle points of contact and a consequent lower capillary penetrability. Indirect support for this interpretation is that the same two-stage penetration pattern was observed on heated CPVC polymer compacts, with the initial slow penetration period progressively extending over a longer time as heating time was prolonged (Carli & Simioni 1980).

CONCLUSIONS

Compression is shown to affect the value of m, the numerical factor in the equation describing the capillary penetration process. As the compaction pressure is increased, m tends to decrease for both the powders. The lowest value (0·095) was obtained for the drug compacts at the highest compaction pressure, which showed a microstructure characterized by a very wide pore size distribution, with no definite peak, shifted towards the smaller pores. On the other hand, the highest m values were found for the polymer compacts prepared at the lowest compaction pressures, which showed a pore size distribution with a sharp and high peak in the larger pore range.

A tentative explanation for the deviation of the m values from the theoretical value of 0·5 given by the Washburn equation, could be that the capillaries are not always parallel, as considered by the Washburn theory, but are interconnected. At the pore network interconnection the following capillary pressure difference exists between pores of different size (Schwartz 1969):

$$\Delta p = 2\gamma \cos\theta \left(\frac{1}{r} - \frac{1}{R}\right)$$

where γ = surface tension of liquid, θ = solid/liquid contact angle, R and r = capillary radius with R > r.

Thus, at the front of penetration, the smaller capillaries are preferentially filled. This means that both the type of pore size distribution, i.e. the presence of a majority of small or large pores, and the distribution width, i.e. the average pressure difference existing at the interconnections, will influence the kinetics of penetration as indeed found in these drug and polymer compacts.

If we consider the values of the mean yield pressure of the two powders, it is possible to observe that the most relevant variations in the capillary microstructure take place when the applied compaction pressure is higher than the mean yield pressure. In fact, the drug compacts present a very much lower penetration constant K and a lower percentage of pore filling when the compaction pressure is raised above the critical value of the mean yield pressure. On the other hand the polymer compacts exhibit a homogeneous structure only at compaction pressures higher than the mean yield pressure.

Finally, the compression exerts a stronger influence on the constants of penetration and on the pore size distributions of the drug compacts than on those of the polymer compacts; this can be reasonably attributed to the fact that the drug powder densification process is also accompanied by particle fragmentation. In fact the B.E.T. surface areas of the drug compacts (Sorptomatic, Kripton Unit, Carlo Erba Strumentazione, Italy) showed a progressive increase up to a final measured area, at 508·3 MN m^{-2}, 30% greater than the initial surface area of the powder.

Although great care must be taken in generalizing these results, it seems reasonable to conclude that

capillary penetration measurements can give useful information in the understanding of the behaviour of pharmaceutical powders under compression.

Acknowledgements

The skilful technical assistance of Messrs A. Capoccia and A. Motta is greatly appreciated. The authors acknowledge Dr V. Mandelli and Mrs N. Orlando, Biometrics Department, Research Development, Farmitalia Carlo Erba, for the statistical analysis of data.

REFERENCES

Ahmed, M., Enever, R. P. (1978) Pharm. Acta Helv. 53: 358–364

Carli, F., Simioni, L. (1979) J. Pharm. Pharmacol. 31: 128

Carli, F., Simioni, L. (1980) Int. J. Pharm. Tech. Prod. Mfg, in press

Couvreur, P., Gillard, J., Roland, M. (1976) Ann. Pharm. Franc. 34 : 123–132

Ganderton, D. (1969) J. Pharm. Pharmacol. 21: Suppl. 9S–18S

Groves, M. J., Alkan, M. H. (1979) Ibid. 31: 575–576

Heckel, R. W. (1961) Trans. Metall. Soc. AIME 221: 671–675

Heertjes, P. M., Kossen, N. W. F. (1967) Powder Technol. 1: 33–42

Hersey, J. A., Rees, J. E. (1970) 2nd Particle Ann. Conf., Bradford

Hoyland, R. W., Field, R. (1976): Paper Techn. Ind. 17: 304–306

Lerk, C. F., Bolhuis, G. K., De Boer, A. K. (1979) J. Pharm. Sci. 68: 205–211

Nogami, H., Fukuzawa, H., Nakai, Y. (1963) Chem. Pharm. Bull. 11: 1389–1398

Orr, C. (1969/70). Powder Technol. 3: 117–123

Palmer, H. K., Rowe, R. C. (1974) Ibid. 9: 181–186

Rode, A. A. (1969) Theory of Soil Moisture, Vol. I, Israel Program for Scientific Translation, Jerusalem, pp 382–384

Samyn, J. C., Yung, W. J. (1970) J. Pharm. Sci. 59: 169–174

Schicketanz, W. (1974) Powder Technol. 9: 49–52

Schwartz, A. M. (1969) Ind. Eng. Chem. 61: 10–21

Sixsmith, D. (1977) J. Pharm. Pharmacol. 29: 82–85

Snedecor, G. W. (1964) Statistical Methods, Iowa State Univ. Press, pp 160–163

Washburn, E. D. (1921) Phys. Rev. 17: 374–392

Winer, J. (1962) Statistical Principles in Experimental Design. McGrow-Hill, New York, pp 46–47

York, P., Pilpel, N. (1973) J. Pharm. Pharmacol. 25, Suppl. 1P–11P